Theoretical Description of Solvent Effects on Fluorescence Spectra of Bulky Charge Transfer Compound DMA-DMPP

ANDREAS B. J. PARUSEL,[1] RUDOLF SCHAMSCHULE,[1] GOTTFRIED KÖHLER[1,2]

[1]*Institute of Theoretical Chemistry and Radiation Chemistry, University of Vienna, Althanstr. 14, 1090 Vienna, Austria*

[2]*Austrian Society for Aerospace Medicine, ISB Institute for Space Biophysics, 1090 Vienna, Austria*

Received 9 April 1998; accepted 2 June 1998

ABSTRACT: Several theoretical models are compared to reproduce the spectroscopic fluorescence shift of 4-(4′-*N*,*N*-dimethylaminophenyl)-3,5-dimethyl-1,7-diphenyl-bis-pyrazolo-[3,4-b;4′,3′e]-pyridine (DMA-DMPP) in different solvents. DMA-DMPP is used as a model compound because it shows a large shift in emission energy for solvents of various polarities and dual fluorescence in polar protic solvents. Although the simple Onsager model is not able to reproduce the experimental results, the self-consistent reaction field (SCRF) model with extension to excited states based on the AM1 Hamiltonian yields excellent agreement. According to the latter model, the red-shifted emission band can be related to a highly polar charge transfer state without geometrical rearrangements, whereas the normal (short wavelength) emission is attributed to emission from an excited state with increased conjugation in a flattened geometry. A supramolecular approach with six molecules of water surrounding the solute can explain satisfactorily the two distinct fluorescence bands. In protic solvents, the emitting CT state shows additional stabilization of the locally excited state with a planar conformation. © 1998 John Wiley & Sons, Inc. J Comput Chem 19: 1584–1595, 1998

Keywords: semiempirical calculations; excited states; solvent effects; fluorescence; charge transfer

Correspondence to: A. B. J. Parusel; e-mail: andreas@majestix.msp.univie.ax.at

Contract/grant sponsor: Fonds zur Förderung der wissenschaftlichen Forschung in Österreich, contract/ grant number; P 11880-CHE

CCC 0192-8651 / 98 / 141584-12

Introduction

Computational methods predict molecular properties and dynamics mainly in the gas phase at 0 K, although most of the processes investigated experimentally occur in condensed media. It is a great challenge to develop sophisticated quantum mechanical methods for the description of solvent effects. As a large number of interactions between the solute ($\mathscr{M}$) and the solvent ($\mathscr{S}$) molecules have to be taken into account, this process is most difficult in many cases.[1] In general, the solvent might introduce significant changes in the electronic and geometric structure of the solute. This becomes especially important for compounds with long range charge separations due to the stabilization of their polar structure by a polarizable environment and the effect of the solvent polarity is able to revert the stability of different conformations of $\mathscr{M}$ in the gas phase and even in nonpolar solvents.[2] An increase in the dipole moment μ of up to 30% compared with gas phase values is found for polar neutral molecules in solution.[3,4] The reactivity in general and particularly the reactive site of the molecule will be affected by the $\mathscr{S}$–$\mathscr{M}$ interactions as well. The enthalpy of chemical reactions and thus their thermodynamics and kinetics are affected by the environment.[5] Reaction coordinates that correspond to a transition state in the gas phase might describe an equilibrium geometry for solvated systems.[6]

Specific interactions might also show strong effects and have to be treated by specific methods. The important hydrogen bond interactions cannot be reproduced satisfactorily without taking into account the effect of the environment describing these specific noncovalent interactions. Computations based on a supramolecular approach alone often result in an insufficient description of the systems investigated. A typical example is the formation of an H-bonded 1:1 complex by two matching nucleic acid bases, which is exothermic in the gas phase. In aqueous solution, each nucleic acid base is solvated by water molecules and no complex formation occurs.[7]

In addition to organic and biochemical reactions, photophysical processes also generally depend on the solvent. Absorption and emission of photons in solution are processes with the charge distribution of the solute $\mathscr{M}$ changing much faster than the orientation of the solvent molecules $\mathscr{S}$. The polarization of the solvent is in equilibrium with the charge distribution of the solute in the electronic ground state. After electronic excitation, a nonequilibrium state is generated, because the electronic polarization of $\mathscr{S}$ is able to reorient nearly instantaneously, whereas the polarization of the dipole moments of $\mathscr{S}$ still corresponds to the electronic ground state. The difference in energy between the equilibrium and nonequilibrium conditions corresponds to the outer reorganization energy and explains the difference between the excitation energies for gas phase and solvated systems. An analogous explanation can be given for the fluorescence process where the energy necessary to produce the nonequilibrium situation of the ground state yields a red-shifted fluorescence in solution in comparison to the emission wavelength in the gas phase. Due to a highly polar or ionic excited state, numerous compounds are strongly influenced by the polarity and viscosity of the solvent after electronic excitation. The natural photosynthetic reaction center of chlorophyll, for instance, is stabilized after photochemical excitation by sunlight via long-range charge separation, creating an intramolecular zwitterion. The spectrum corresponds to a long-term excited state caused by a hindered back-electron transfer (BET).[8]

Several organic molecules of general donor–acceptor (D–A) structure, separated by a conjugated π-system (spacer) are subject to a partial intramolecular charge transfer (ICT) process after absorption of radiation.[9–11] The excited state of charge transfer character may be stabilized (similar to the photosynthetic reaction center) by decoupling the donor and the acceptor subunits. These two steps—charge transfer and the decoupling via rotation about the single bond connecting the donor and acceptor subunits—lead to the so-called twisted intramolecular charge transfer (TICT) state.[12,13] A significant rise of the red shift in fluorescence and a rise in dipole moment μ of the excited state are found with increasing chain length of the spacer separating D and A, because of an enlarged charge separation. Several long μ-conjugated systems substituted with both a strong electron donor and acceptor show nonlinear optical (NLO) properties, as recently shown.[14] These NLO effects are of major importance because they are fundamental for optical processing, for storage of data (e.g., optical disk storage), and for images (e.g., read- and writeable holograms). Compounds with hyperpolarizable properties are rare and crucial for future communication systems and com-

puters. The fluorescence behavior and the nonlinear properties of donor–spacer–acceptor systems also show a strong dependence on the polarity and viscosity of the solvent $\mathscr{S}$, because highly polar excited states are formed.

4-(4′-*N*,*N*-dimethylaminophenyl)-3,5-dimethyl-1,7-diphenyl-bis-pyrazolo-[3,4-b;4′,3′e]-pyridine (DMA-DMPP, see Fig. 1) is an interesting molecule with respect to the above mentioned items. This donor–acceptor compound has been synthesized[17] and studied with semiempirical methods[18,19] to investigate the theories of charge transfer processes. In the course of these characterizations, DMA-DMPP, with its enlarged μ-system (the distance from the methyl carbon atom to the phenyl carbon atom on the opposite side of the compound is about 14 Å) is most important for the subsequent investigation of its nonlinear properties as well as for representing a model system of a multistep electron transfer with a long-living charge-separated system comparable to the photosynthetic reaction center. The excited state of DMA-DMPP exhibits a charge separation yielding a large Stokes shift for various polar solvents. In addition, a second emission band arises for polar and protic solvents.

Semiempirical calculations in the gas phase[19] give evidence of a highly polar excited state S_6 with a dipole moment of 26 D. In this state, the dimethylanilino (DMAn) donor and the bis-pyrazolo-pyridine (BPP) acceptor are decoupled by a torsional angle of 90°. Only a small geometrical rearrangement of the ground state conformation pretwisted by 81° is necessary to achieve this perpendicular arrangement of the subunits. No stabilization is found for a more coplanar orientation of the subunits in the ground and the excited states due to the strong sterical hindrance of the two bulky methyl groups in the 3- and 5-position. For a rotation of the DMAm group about the single bond connected to the phenyl group the DMAm moiety can be denoted as the donor group. The gas phase calculations also yield a perpendicular twisted intramolecular charge transfer state S_3 with a dipole moment of 16.8 D, which is attributed to a complete charge transfer from the free electron pair of the nitrogen to the phenyl group. No unequivocal assignment to the fluorescing state of DMA-DMPP could be done with the gas phase computations because of the large solvent effects. Additional information is necessary whether the intramolecular charge transfer state of higher energy (S_6) with a large dipole moment of 26 D will be energetically stabilized in solution below the twisted intramolecular charge transfer state (S_3). This TICT state has a smaller dipole moment but is lower in total energy. Thus, especially the dual fluorescence in the polar, protic environment cannot yet be explained so far, because two distinct local minima must be localized in the emission excited state.

In the present study, a detailed semiempirical study of the excited states of DMA-DMPP is presented. Two decisive rotational modes are identified to explain its unusual emission spectrum. The solvent models of Onsager, the self-consistent reaction field approach, and a supermolecule formation are analyzed and compared with the experimental results.

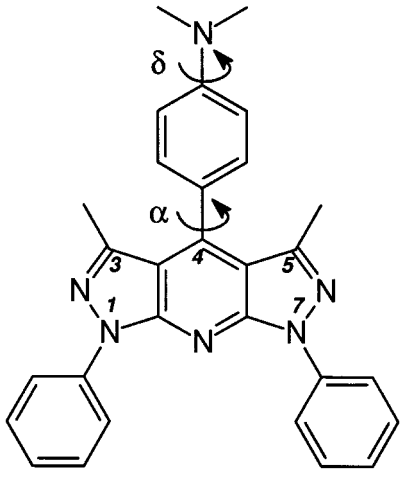

FIGURE 1. Structure of DMA-DMPP with definition of rotation angles α and δ.

Computational Methods

COMPUTATIONAL PROCEDURE

The complete AM1-optimized[20] geometries of the electronical ground state given in a previous work[18] are used as starting geometries. The torsion angles about the dimethylamino-bis-pyrazolo-pyridine single bond (α) and rotation of the dimethylamino group about the single bond connecting the phenyl-bis-pyrazolo-pyridine moiety (δ) (for the definition of the angles see Fig. 1) have been found to be 81° and 0°, respectively, for the ground state structure in gas phase. The slight pyramidalization at the dimethylamino group and the twist of the two phenyl groups in the 1- and 7-position of 41° can be neglected[18] and will not be taken into account in further computations. The

rotational angle α was varied in steps of 10° from 90° down to 40°, whereas the twisting angle δ was varied from a planar ($\delta = 0°$) to a perpendicular conformation ($\delta = 90°$) in 15° steps.

The commercial semiempirical program package VAMP, version 6.1,[21] is used for all computations and the visualization of the molecular properties is obtained by TRAMP, version 1.1.[22] All calculations are performed on SGI INDY workstations (MIPS R4400) at the University of Vienna. The solvated excited state energies and dipole moments are obtained using ground-state-optimized geometry with configuration interaction including all single and double excitations from each of the five highest occupied orbitals to the five lowest unoccupied orbitals (CISD = 10). This choice of the active space has been the subject of a detailed characterization given elsewhere.[19]

ONSAGER MODEL

The Onsager model was first described by Lars Onsager in 1936.[23] The solvent $\mathscr{S}$ is treated as a dielectric continuum without a specific structure. The solute $\mathscr{M}$ is embedded in a spherical cavity with the so-called Onsager radius a. The nonspecific interactions $\mathscr{S}$-$\mathscr{M}$ are characterized by macroscopic properties of the solvent, the dielectric constant ε and the refractive index n. The solvation energy for the electronic ground state is calculated using Onsager's formula for a fully relaxed state[24]:

$$\Delta E_{solv,\,fully} = -\frac{2\mu_i^2}{4\pi\varepsilon_0 a^3}\frac{\varepsilon - 1}{2\varepsilon + 1}$$

where ε_0 is the universal dielectric constant, ε the dielectric constant of $\mathscr{S}$, a the Onsager cavity radius, and μ_i the dipole moment of the fully equilibrated state. The solvation energies for the excited states are calculated using the formula for a partially solvated state assuming that the change in the dipole moment of $\mathscr{M}$ from the initial value μ_i to a final amount μ_f occurs so rapidly that the solvent molecules do not have enough time for reorientation[25]:

$$\Delta E_{solv,\,partial} = -\frac{2\mu_f\mu_i}{4\pi\varepsilon_0 a^3}\left(\frac{\varepsilon - 1}{2\varepsilon + 1} - \frac{n^2 - 1}{2n^2 + 1}\right) - \frac{2\mu_f^2}{4\pi\varepsilon_0 a^3}\frac{n^2 - 1}{2n^2 + 1}$$

Here, n is the refractive index of the solvent $\mathscr{S}$. The stabilized total energies are obtained by addition of the solvent energy ΔE_{solv} and the gas phase energies. For all calculations of solvation energies, a cavity radius of 6.26 Å is used such as that obtained for the solvent-accessible radius by VAMP calculations. Half the distance between a dimethylamino carbon atom and the most distant phenyl carbon atom was calculated to be 6.8 Å. Thus, the smaller radius of the cavity causing a strengthened solvent effect will be obtained with our results. The calculations have been carried out using acetonitrile as a polar and nonprotic continuum solvent with $\varepsilon = 37.5$ and $n = 1.344$.

SELF-CONSISTENT REACTION FIELD THEORY

In the numerical self-consistent reaction field (SCRF) model for ground and excited states in an AM1-based method,[26] the solvent is treated as a dielectric polarizable continuum characterized by its dielectric constant ε and its refractive index n analogous to the Onsager model. The polarization of the continuum generates an electrostatic field, the so-called reaction field, which polarizes the solute $\mathscr{M}$ within the cavity. This process is brought to self-consistency by a normal self-consistent field (SCF) iteration sequence.

Within this method an enlarged van der Waals cavity is fitted to the molecule (see Fig. 2). The surface of the cavity is divided into sections with partial spheres and the electric field of $\mathscr{M}$ is computed at the origin of each sphere. The free energy of solvation is computed as the sum of three contributions according to:

$$\Delta G_{tot}^{solv} = \Delta G_{estat}^{solv} + \Delta G_{disp}^{solv} + \Delta G_{cav}^{solv}$$

where ΔG_{estat}^{solv} is the electrostatic interaction of $\mathscr{M}$ with the induced reaction field of the solvent cage, ΔG_{disp}^{solv} the dispersion interaction of $\mathscr{M}$ with $\mathscr{S}$ and ΔG_{cav}^{solv} the free cavity energy necessary to generate the solvent cage in the continuum. It has been shown[26] that ΔG_{disp}^{solv} and ΔG_{cav}^{solv} are of the same magnitude, but of opposite signs for both large polar solutes and solvent molecules, and thus their sum can be neglected in most cases. DMA-DMPP is a spherical polar molecule and has been investigated chiefly in the polar environment. Therefore, only the electrostatic contribution is taken into account. The nonequilibrium effects in electronic excitation and emission, as described in the Introduction, are explicitly considered within the reaction field approach. Therefore, both the calculated absorption and fluorescence energies are corrected

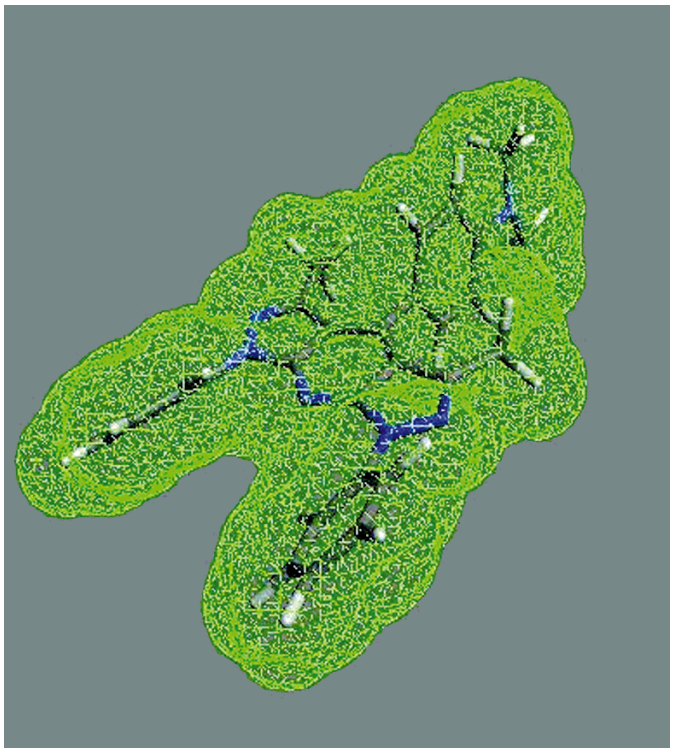

FIGURE 2. Schematic representation of DMA-DMPP van der Waals' cavity shape within the numerical SCRF model.

with respect to these kinds of nonequilibrium effects in the multitude of excited states.

SUPRAMOLECULAR APPROACH

For the generation of the supramolecule,[27] six molecules of the solvent water are added to the DMA-DMPP solute. With this approach, specific $\mathscr{S}$-$\mathscr{M}$ interactions such as hydrogen bonding can be estimated successfully. The four nitrogen free electron pairs are most likely the sites for formation of the stable hydrogen bonded complexes. The six molecules of water are placed arbitrarily at different sites in relation to DMA-DMPP and optimized in geometry independently. Due to the large solvent-accessible surface at the dimethylamino group, three molecules of water are located around this subunit.

The most stable conformation is presented in Figure 3. The optimized geometry remains almost unchanged, just the small pyramidalization of the dimethylamino group vanishes. The complex of solvent molecules and DMA-DMPP with a planar dimethylanilino results as the geometry of lowest energy.

Results and Discussion

ONSAGER MODEL

The stabilization energies of the excited states of DMA-DMPP in solution are calculated for both rotations α (dimethylanilino group) and δ (dimethylamino group). The dipole moments are summarized in Table I. The evolution of total energy as a function of the rotational mode α is given for both the Onsager model (Fig. 4a) and the gas phase (Fig. 4b) according to ref. 19.

Due to their small dipole moment, the first and second excited states of local excited (LE) character are hardly affected by the solvent. S_2 with $\mu = 1.3$ D at $\delta = 0°$ and $\alpha = 90°$ is stabilized by only 0.2 kcal/mol, whereas the other LE state, with an average dipole moment of 8 D ($\alpha = 60°$), is stabilized by 2.5 kcal/mol. The small stabilization of more coplanar structures (decreasing α) is clearer for the first excited state than for S_2, as shown in Figure 4b. Due to the larger increase of the S_2 dipole moment along this α-coordinate, a nearly isoenergetic behavior for S_1 and S_2, according to the Onsager model, can be seen in Figure 4a. The

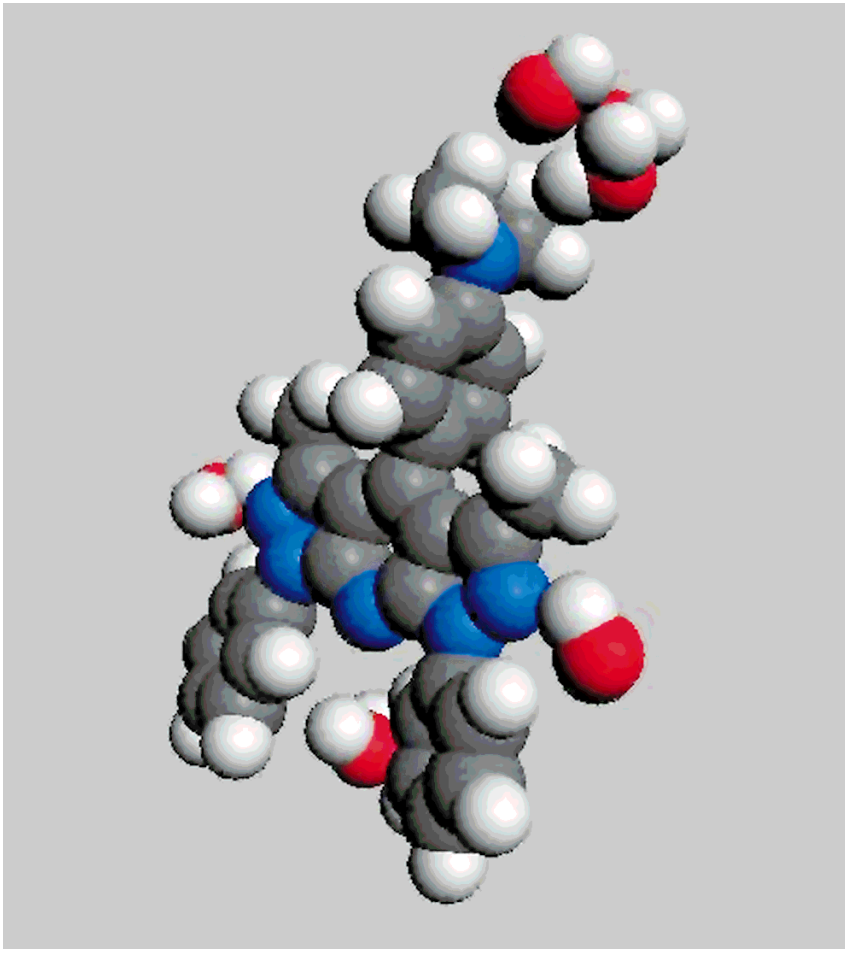

FIGURE 3. Optimized structure of the DMA-DMPP:6 H_2O complex according to the supramolecular formulation.

third and fourth excited states of A_1 and B_2 symmetry with an average decrease of 3–4 D in dipole moment along the rotation coordinate are not influenced by the solvent. The destabilization for small angles α remains similar in comparison to gas phase destabilization. For the intramolecular charge transfer excited state S_{CT}, the donor is located on the dimethylanilino and the acceptor on the bis-pyrazolo-pyridine subunit, respectively. This state is the third excited state in the gas phase (see Fig. 4b; for clarity, only the excited states examined are shown in Fig. 4) for small rotation angles α ($\alpha \leq 60°$) and is destabilized to become the sixth excited state for $\alpha \leq 70°$. The very large dipole moment of S_{CT} ($\mu = 26.5$ D at $\alpha = 90°$) shows a large solvation energy of 17.9 kcal/mol.

TABLE I.
Gas Phase Dipole Moment μ (in D) of DMA-DMPP Excited States for Several Conformations.

	$\alpha = 40°$ $\delta = 0°$	$\alpha = 90°$ $\delta = 0°$	$\alpha = 90°$ $\delta = 90°$
$\mu(S_1, LE)$	9.1	4.5	1.9
$\mu(S_2, LE)$	1.3	1.3	4.1
$\mu(S_3, A_1, TICT)$	3.4	7.6	16.8
$\mu(S_4, B_2)$	5.1	8.2	13.6
$\mu(S_6, A_1, CT)$	9.0	26.5	31.5

Nevertheless, this excited state is still disfavored in energy by more than 6 kcal/mol in comparison to the first excited state. This highly polar charge transfer state is not stabilized below the two LE states S_1 and S_2 and is not the fluorescing state. The dipole moment of this state remains almost constant along the twisting coordinate δ ($\mu = 26.5$ D for $\mu = 0°$ and $\mu = 31.5$ D for $\delta = 90°$) and no significant change in the ordering of the

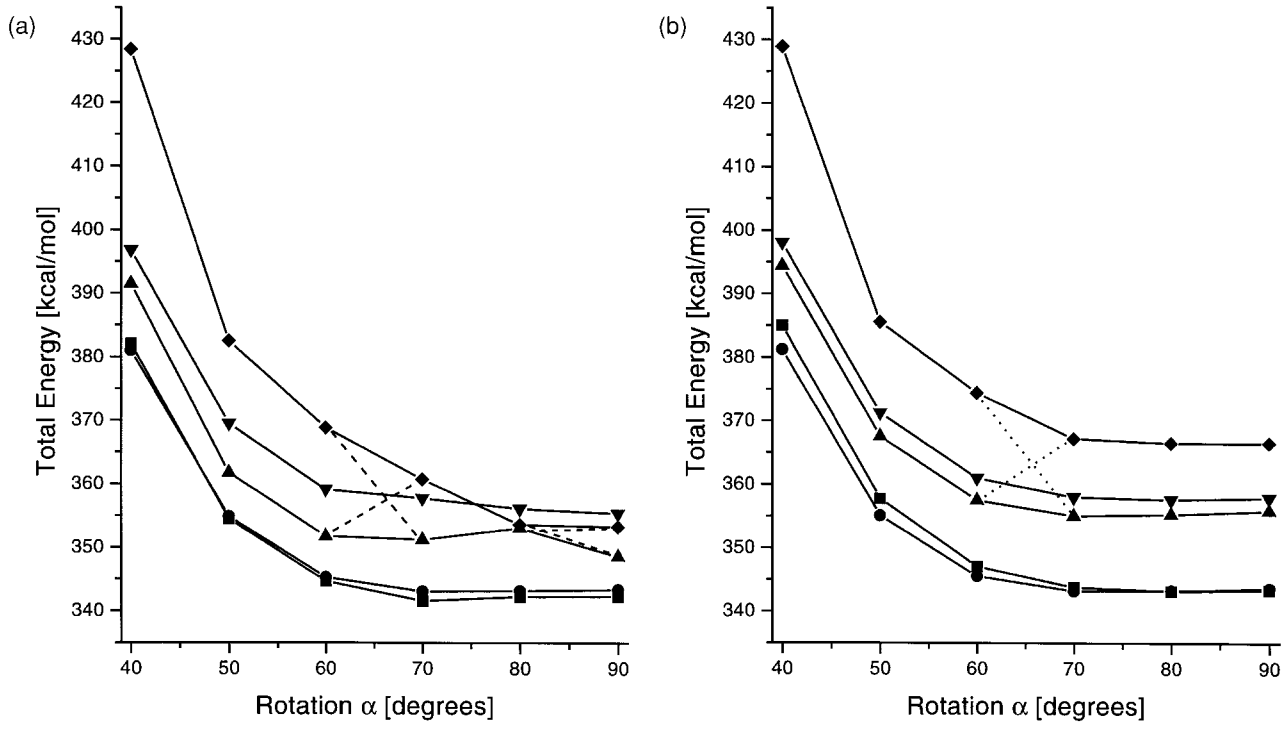

FIGURE 4. Variation of S_1 (■), S_2 (●), S_3 (S_{TICT}, A_1 symmetry) (▲), S_4 (B_2 symmetry) (▼), and S_{CT} (♦) total energy of DMA-DMPP as a function of rotation angle α according to the (a) Onsager formulation and for (b) the gas phase.

solvated excited state is caused for S_{CT} along δ. The third excited state S_3, however, increases its dipole moment from $\delta = 0°$ to $\delta = 90°$ by approximately 10 D (see Table I) and its solvation energy is clearly affected upon twisting of the dimethylamino group. The main contribution of this donor–acceptor decoupled transition ($\delta = 90°$) consists of a complete charge transfer from the free electron pair of the nitrogen to the directly connected phenyl moiety. ΔG_{solv} is calculated to be about 7 kcal/mol ($\delta = 90°$), but energetically remains above the first excited state [$\Delta H(S_1) =$ 347.2 kcal/mol and $\Delta H(S_{TICT}) = 350.5$ kcal/mol]. Both the twisted intramolecular charge transfer state and the highly polar ICT state (S_6 in gas phase), as the origin of the red-shifted fluorescence, are excluded by the solvent calculations according to the Onsager model. This highly approximate model is thus generally unable to explain the fluorescence behavior of DMA-DMPP in polar solvents such as acetonitrile. A stabilization of the S_{CT} can be detected, but the total amount of stabilization is not sufficient to localize the S_{CT} as the first excited state.

SCRF THEORY

The electronic ground state and excited states of DMA-DMPP as a function of the rotational angle α and twisting angle δ are investigated. The total energies, as obtained by the SCRF-CI calculations in acetonitrile, are presented in Table II and Figure 5. The ground-state energies in solution differ from those in the gas phase. The increase in energy for planarization to $\alpha = 40°$ is computed to be 6 kcal/mol in the gas phase,[18] whereas an increase in energy of 39.5 kcal/mol results for DMA-DMPP

TABLE II.
Dipole Moments μ (in D) of DMA-DMPP Excited States in Acetonitrile for Several Conformations According to SCRF-CI Calculations.

	$\alpha = 40°$ $\delta = 0°$	$\alpha = 90°$ $\delta = 0°$	$\alpha = 90°$ $\delta = 90°$
$\mu(S_1, LE)$	17.0	5.8	3.3
$\mu(S_2, LE)$	6.4	0.2	2.7
$\mu(S_3, A_1, TICT)$	6.8	4.0	21.8
$\mu(S_4, B_2)$	4.5	7.5	1.0
$\mu(S_6, A_1, ICT)$	3.9	30.3	30.6

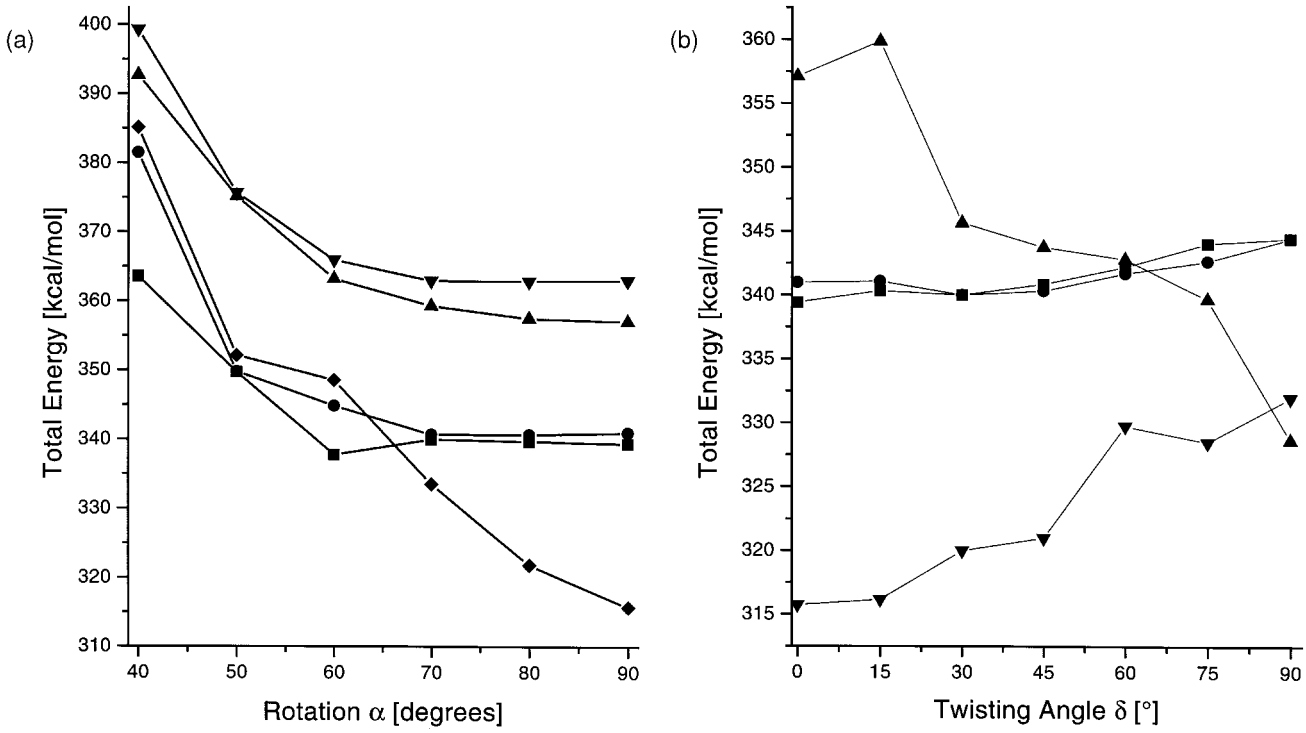

FIGURE 5. Variation of S_1 (■), S_2 (●), S_3 (S_{TICT}, A_1 symmetry) (▲), S_4 (B_2 symmetry) (▼), and S_{CT} (♦) total energy of DMA-DMPP as a function of rotation angle α (a) and twisting angle δ (b) in acetonitrile according to SCRF-CI results.

in acetonitrile. The free solvent-accessible surface between the methyl groups in the 3- and 5-positions and the perpendicular dimethylamino unit are filled up with the solvent continuum. For the S_0, the energy barrier for rotation into a more planar conformation is high. Consequently, the energetical minimum is located at $\alpha = 90°$ in contrast to the gas phase where $\alpha = 81°$ is the total minimum conformation. Different results are also obtained with regard to δ. The conformation with $\delta = 30°$ is stabilized by 1.5 kcal/mol versus the planar geometry, which is the minimum in gas phase. Interactions of the solvent with the NMe_2 group weaken the conjugation of the nitrogen lone pair and allow a slight torsion δ of the amino group caused by steric hindrance between the methyl and *o*-phenyl hydrogen atoms [d(H—H) = 2.4 Å].

The stabilization of the highly polar charge transfer state is quite large (see Fig. 5), which is predominantly due to $\mathcal{S}$-$\mathcal{M}$ interactions. This excited state is the first excited state for enlarged decoupling of the dimethylanilino and bispyrazolo-pyridine subunits ($\alpha \leq 70°$) and for almost all twisting angles δ. At $\delta = 90°$, the S_{CT} is located 3.3 kcal/mol above the S_1. The dipole moment increases (see Tables I and II.) from 26.5 D in the gas phase to 30.3 D in acetonitrile and synergistically strengthens the effect of stabilization. A significant charge transfer from the donor to the acceptor moiety can be seen unequivocally as well as a very large increase in dipole moment for the charge transfer state. The total free energy of solvation is calculated to 39.5 kcal/mol. The dipole moment of the first excited state (LE) increases rapidly upon flattening. For $\alpha = 40°$, the value of 17.0 D leads to a large contribution of ΔG_{tot}^{solv} to the total energy of S_{LE}. This state becomes the first excited state, whereas, for $\alpha = 90°$, the comparatively small dipole moment of 5.8 D causes no evident stabilization. For the twisted intramolecular charge transfer excited state the dipole moment increases significantly [see Table II: $\Delta\mu = \mu(\delta = 90°) - \mu(\delta = 0°) = 17.8$ D], yielding a continuous decrease in total energy upon increasing δ. For perpendicular subunits, the TICT state becomes the first excited state. A comparison of destabilization of energy in the gas phase upon dimethylamino group twisting between the S_{CT} (S_6) and S_{TICT} (S_3) results in a much stronger increase in energy for S_{CT} compared with S_{TICT}. Thereby, the comparatively small dipole moment ($\mu_{TICT} = 21.8$ D, whereas $\mu_{CT} = 30.6$ D) yields a more efficient lowering in energy of the TICT

state, which becomes the first excited state for $\delta = 90°$. Nevertheless, a relaxation of DMA-DMPP in its excited state does not go along with any geometrical rearrangements according to our calculations. The first excited state S_{CT} is populated after excitation and an increase in total energy for both α and δ prevents any twisting or rotational motions. The coordinate α shows a barrier of approximately 13 kcal/mol upon twisting before the $\delta = 90°$ TICT state is able to become the first excited state.

The results of the SCRF-CI calculations of energies for several decisive conformations are summarized in Table III. The fluorescence energies differ somewhat from the energy gap $\Delta\Delta H = \Delta H(S_n) - \Delta H(S_0)$, because the destabilization in energy is taken into account, caused by the nonequilibrium situation after emission of fluorescence. An excellent agreement of experiment (ν_{fl} = 552 nm) with the calculation (ν_{fl} = 573 nm for $\alpha = 90°$ and $\delta = 0°$) is found. Thus, the fluorescence of DMA-DMPP in polar solvents occurs out of a decoupled intramolecular charge transfer state S_{CT} without any geometrical relaxation. In addition, a slightly different situation is found for the fluorescence out of a hypothetical S_1 TICT ($\delta = 90°$) state. The destabilization of the ground state at $\delta = 90°$ is taken into account by a nonequilibrium situation. ν_{fl}(TICT) is energetically less favored in contrast to the ν_{fl}(CT). The wavelength ν_{fl}(TICT) becomes 423 nm, whereas ν_{fl}(CT) is 440 nm.

Subsequently, the calculated fluorescence energies are compared with the experimental results obtained by Rotkiewicz et al.[17] In Table IV, the intramolecular charge transfer state emission energies for $\alpha = 90°$ are given in comparison to experiment. The solvation effects are shown for a series of different solvents with hexane as the most apolar and water as the most polar solvent. Additionally, in Figure 6, a Lippert–Mataga plot is given with the emission energies as a function f_1 of the refractive index n and the dielectric constant ε according to:

$$f_1 = \frac{\varepsilon - 1}{2\varepsilon + 1} - \frac{1}{2}\frac{n^2 - 1}{2n^2 + 1}$$

The experimental results are represented best by two distinct linear fits, whereas the theoretically obtained results for the perpendicular charge transfer emission (S_{CT}, $\alpha = 90°$), as well as the fluorescence out of the lowest LE state with $\alpha = 90°$ and $\alpha = 60°$, respectively, are characterized fairly well by a single linear fit. The shift in emission out of the perpendicular ($\alpha = 90°$) and more

TABLE III.
Calculated Fluorescence Energies ν_{fl}^{SCRF} (in nm) of DMA-DMPP in Acetonitrile for Several Conformations.

	$\alpha = 40°$ $\delta = 0°$	$\alpha = 90°$ $\delta = 0°$	$\alpha = 90°$ $\delta = 90°$
$\nu_{fl}(S_1, LE)$	419	328	315
$\nu_{fl}(S_2, LE)$	311	324	318
$\nu_{fl}(S_3, A_1, TICT)$	266	258	423
$\nu_{fl}(S_4, B_2)$	286	273	259
$\nu_{fl}(S_6, A_1, ICT)$	319	573	440

TABLE IV.
Experimentally Obtained (ν_{fl}^{exp}) and Calculated (ν_{fl}^{SCRF}) Fluorescence Energies of DMA-DMPP (in nm) in Various Solvents with Deviations in Percentage of Calculated versus Experimental Emission Energies.[1]

	ν_{fl}^{exp}	ν_{fl}^{SCRF}	Deviation
Hexane	429	316	+35.5
Benzene	437	326	+34.0
Methylenchloride	474	492	−3.5
DMSO	568	543	+4.5
Enthanol	556	548	+1.5
Acetonitrile	552	573	−3.5
Methanol	575	576	±0
Water	—	591	

[a] Theoretical values correspond to $\alpha = 90°$ ICT emission.

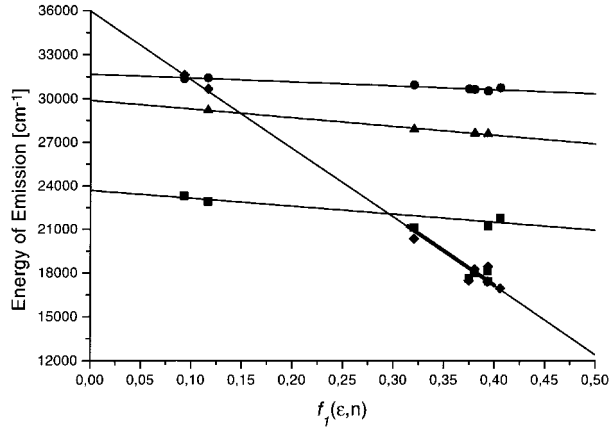

FIGURE 6. Lippert–Mataga plot of DMA-DMPP of experimentally observed (—■—) and calculated (ICT state at $\alpha = 90°$ (♦), S_1 LE at $\alpha = 90°$ (●) and $\alpha = 60°$ (▲)) fluorescence energies in various solvents. The solvents considered include, from left to right, hexane, benzene, methylenchloride, DMSO, ethanol, acetonitrile, methanol, and water.

planar ($\alpha = 60°$) LE conformation agrees quite well with the experimental results. For the dual-fluorescence phenomenon in water and alcohols the short wavelength emission (attributed to a LE emission) is considered. A decrease in energy can be seen for more planar conformations (approximately 2000 cm^{-1}).

Due to the parallel course of experimental and theoretical LE graphs, the short wavelength emission of DMA-DMPP in apolar solvents can be attributed to an emission out of a flattened conformation in the local excited state. Thus, the experimentally obtained small solvent shift can be predicted by our calculations. The deviation of approximately 30% from the experimental value may be attributable to the use of the CISD method. As mentioned before, the two terms, ΔG_{disp}^{solv} and ΔG_{cav}^{solv}, are neglected by our calculations. However, these contributions could become of major importance for an apolar environment like hexane or benzene. In addition, the choice of a semiempirical AM1 wave function is probably the largest source of error in the calculations.

To explain the planarization of the solute $\mathscr{M}$, a series with SCRF-CI calculations in *n*-hexane as solvent were carried out. In Figure 5, a local minimum in acetonitrile for the planar ($\alpha = 60°$) conformation of the first LE (S_1) is found. Nevertheless, this excited state minimum [$\Delta H_{LE}(\alpha = 90°) - \Delta H_{LE}(\alpha = 60°) = 3.4$ kcal/mol] does not play a decisive role in polar solvents, because the charge transfer state is energetically stabilized far below this local minimum, which cannot be reached. For apolar media the situation has to be described from a different point of view. In Figure 7, the first and second excited state in n-hexane are presented along the rotation coordinate α. In this solvent, no highly polar charge transfer state is shifted energetically below the LE states (S_1 and S_2). The LE is stabilized by rotation about the dimethylanilino—bis-pyrazolo-pyridine single bond to the global excited state minimum at $\alpha = 60°$. The transition state at $\alpha = 70°$ is located only 2.2 kcal/mol higher in energy than the local minimum at $\alpha = 80°$, and thus may be passed easily at room temperature. Therefore, in apolar environment fluorescence occurs out of a more planar conformation in the first excited LE state.

In contrast, the experimental and theoretical values for polar solvents agree very well even in absolute numbers (maximal deviation 4.5%) compared with the intramolecular charge transfer emission for orthogonal moieties ($\alpha = 90°$). For all polar solvents, the highly polar intramolecular charge transfer state is stabilized significantly and becomes the emitting state. Because the slopes of both the experimental and theoretical plot are identical, the solvent shift for DMA-DMPP in polar solvents can be predicted.

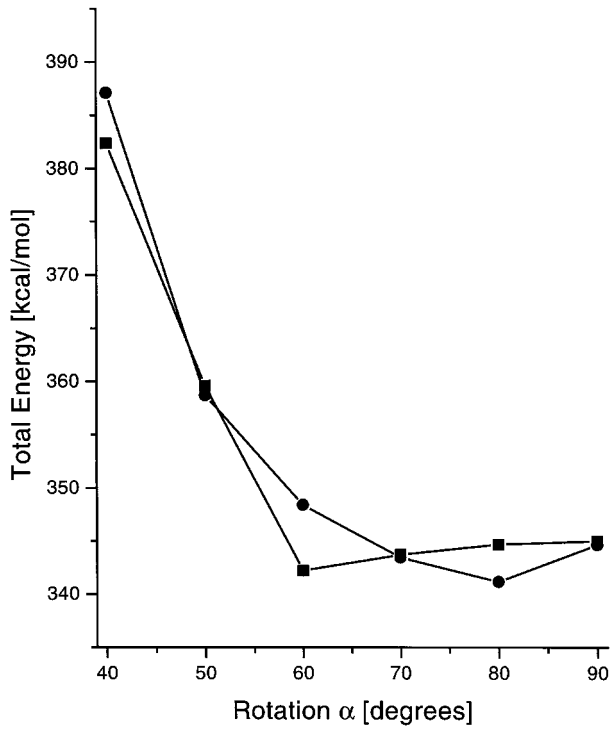

FIGURE 7. Variation of S_1 (■) and S_2 (•) total energy of DMA-DMPP as a function of rotation angle α in *n*-hexane according to SCRF-CI results.

SUPERMOLECULE APPROACH

For the explanation of dual fluorescence in polar, protic solvents, the models just discussed are not satisfactory, because the most probable effect of a protic solvent is the formation of hydrogen bonds, which are neglected in all continuum models. Thus, a supermolecule approach using six single molecules of water attached to DMA-DMPP may give a more reasonable explanation for the unusual fluorescence behavior.

In Figure 3 the optimized geometry of DMA-DMPP:6 H_2O is shown. Experimental results,[28] as well as our computations, identify the amino group to be the most likely position for hydrogen bonding and/or protonation of DMA-DMPP. The theoretical and experimental aspects of a protonated form of DMA-DMPP will be presented in another work.[29] As can be seen in Figure 3, the pyridine amino atom is sterically hindered from access to a

solvent molecule by the two phenyl groups in the 1- and 7-positions. Even a small water molecule cannot freely approach the nitrogen [optimized distance d(N—H) = 3.6 Å], whereas the distances from the water hydrogen atom to the pyrazolo and the amino nitrogen are 2.7 Å and 3.0 Å, respectively. Nonetheless, six atoms of water are definitely not enough to treat the specific hydrogen bonding interaction sufficiently. Nevertheless, a general trend regarding the evolution of DMA-DMPP in its hydrogen-bonded excited states can be given.

The DMA-DMPP energy with six molecules of a protic solvent attached to it is shown as a function of the rotational angle α in Figure 8. A general stabilization of the planar conformation for α = 50° is obtained for S_1 to S_4, whereas the intramolecular charge transfer state S_{CT} increases slightly in total energy with decreasing angle α. According to this picture, a relaxation of DMA-DMPP occurs via a planarization of the S_1 state of locally excited character. Due to the fact that the dipole moment increases significantly for a more flattened geometry, this trend of planarization will be much more affected in a ''real condensed'' system of DMA-DMPP surrounded by numerous molecules of water. The effect of hydrogen bonding for α = 50° leads to a stabilization of approximately 2.5 kcal/mol [ΔH(α = 90°) = −37.9 kcal/mol; ΔH(α = 50°) = −40.6 kcal/mol]. It has been shown for acetonitrile that the intramolecular charge transfer state is significantly stabilized in polar solvents and a global minimum in S_1 energy results. Additionally, for protic solvents, a second local minimum of DMA-DMPP exists in its locally excited state at α = 50°.

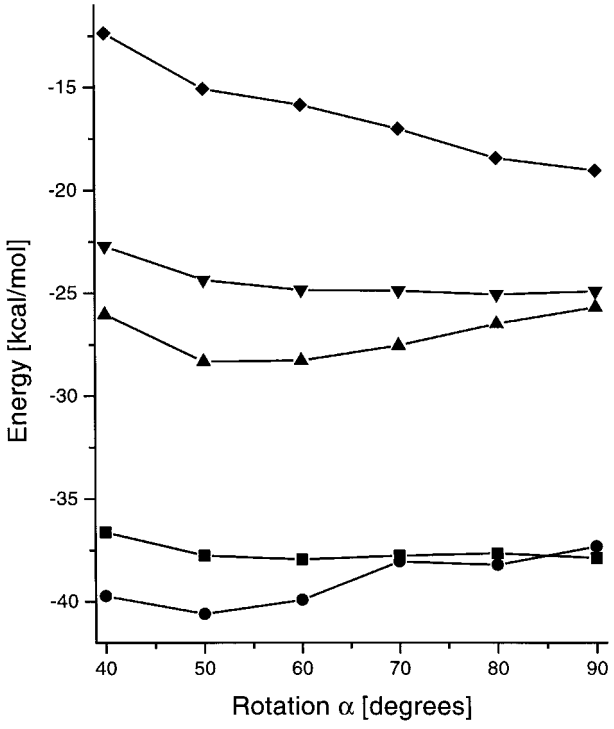

FIGURE 8. Variation of S_1 (■), S_2 (●), S_3 (S_{TICT}, A_1 symmetry) (▲), S_4 (B_2 symmetry) (▼) and S_{CT} (♦) total energy of DMA-DMPP:6H_2O as a function of rotation angle α in acetonitrile.

We therefore propose for DMA-DMPP a modified mechanism for explanation of the dual-fluorescence phenomena in protic solvents. After photoexcitation and vibronic relaxation in the second excited state, an internal conversion (IC) to the first excited state occurs. Due to the conical intersection point at the transition state geometry of S_1, the molecule is able to relax either into the local minimum of the local excited state at α = 50° or into the global excited state minimum at α = 90°.

Conclusion

The theoretical interpretation of the fluorescence spectrum of the bulky charge transfer compound DMA-DMPP has been the main goal of our investigation. Three different models including solvent effects into quantum-mechanical calculations have been used and compared with one another and with the experimental data.

The high polar intramolecular charge transfer state available at perpendicular donor–acceptor subunits (α = 90°) is stabilized in total energy below the two partial charge transfer states, S_3 and S_4 yet not below the two local excited states, S_1 and S_2, which are hardly affected by the solvent continuum as described by the Onsager model. This approach is thus unable to explain the experimental results sufficiently.

The SCRF-CI model shows remarkable agreement with the experiments. Solvent shifts and excited state properties in both polar and apolar solvents can be predicted precisely. In polar solvents the shift in fluorescence is predicted correctly and emission out of the stabilized polar charge transfer state S_{CT} is shown for CH_3CN, whereas emission out of a TICT state can be excluded. The planar conformation of the locally excited state S_1 plays an important role in apolar solvents. Here, a local minimum occurs for α = 60°, which corresponds to an enlarged conjugation over the whole molecule. The gradient of the fitted plot

for this LE emission corresponds to the experimental one and fluorescence out of this conformation can be observed.

In polar protic solvents, where hydrogen bonds may form, the red-shifted emission is attributed to the decoupled ($\alpha = 90°$) CT state, while a significant stabilization of the planar ($\alpha = 50°$) LE state S_1 creates a second energetic minimum with a significant barrier to account for the short wavelength emission.

A large difference in dipole moment for ground to excited state ($\Delta\mu_{eg}$) is a major requirement for the occurrence of large nonlinear optical effects. Especially large donor–acceptor compounds separated by π-conjugated systems are predestined to show NLO properties. The experimental and theoretical study of DMA-DMPP has shown that this system is characterized by a $\Delta\mu_{eg}$ of more than 30 D. Thus, experimental and theoretical studies of DMA-DMPP and its derivatives with enlarged donor–spacer–acceptor structure should be done to explore possible applications.

Acknowledgments

The authors are thankful to Dr. Peter Gedeck and Prof. Krystyna Rotkiewicz for useful discussions, and to Dr. Harald Lanig for disposal of TRAMP. We are indebted to Dr. Rudolf Hutterer and Erich Ruprecht for reading the manuscript.

References

1. J. Tomasi and M. Persico, *Chem. Rev.*, **94**, 2027 (1994).
2. P. Beak, F. S. Fry, J. Lee, and F. Steele, *J. Am. Chem. Soc.*, **98**, 171 (1976).
3. F. J. Luque, M. J. Negre, and M. Orozco, *J. Phys. Chem.*, **97**, 4386 (1993).
4. C. J. Cramer and D. G. Truhlar, *Chem. Phys. Lett.*, **74**, 198 (1992).
5. D. G. Giesen, J. W. Storer, C. J. Cramer, and D. G. Truhlar, *J. Am. Chem. Soc.*, **117**, 1057 (1995).
6. M. Orozco, C. Alhambra, X. Barril, J. M. López, M. A. Busquets, and F. J. Luque, *J. Mol. Model.*, **2**, 1 (1996).
7. L. X. Dang and P. A. Kollman, *J. Am. Chem. Soc.*, **112**, 503 (1990).
8. J. Deisenhofer and J. R. Norris, In *The Photosynthetic Reaction Center, Vols. I. and II*, Academic, New York, 1993.
9. D. Gust, T. A. Moore, and A. L. Moore, *J. Mol. Biol.*, **180**, 385 (1993).
10. M. R. Wasielewski, *Chem. Rev.*, **92**, 435 (1992).
11. W. Rettig, *Angew. Chem*, **98**, 969 (1986); *Angew. Chem. Int. Ed. Engl*, **25**, 971 (1986).
12. K. Rotkiewicz, K. H. Grellmann, and Z. R. Grabowski, *Chem. Phys. Lett.*, **19**, 315 (1973).
13. Z. R. Grabowski, K. Rotkiewicz, A. Siemiarczuk, D. J. Cowley, and W. Baumann, *Nouv. J. Chim.*, **3**, 443 (1979).
14. J.-L. Brédas, *Chem. Rev.*, **94**, 243 (1994).
15. J.-L. Brédas, *Science*, **263**, 487 (1994).
16. S. R. Marder, L-T. Cheng, B. G. Tiemann, A. C. Friedli, and M. Blanchard-Desce, *Science*, **263**, 511 (1994).
17. K. Rotkiewicz, K. Rechthaler, A. Puchała, D. Rasała, S. Styrcz, and G. Köhler, *J. Photochem. Photobiol. A: Chemistry*, **98**, 15 (1996).
18. A. B. J. Parusel, R. Schamschule, D. Piorun, K. Rechthaler, A. Puchała, D. Rasała, K. Rotkiewicz, and G. Köhler, *J. Mol. Struct.* (*THEOCHEM*), **419**, 63 (1997).
19. A. B. J. Parusel, R. Schamschule, and G. Köhler, *Ber. Bunsenges. Phys. Chem.*, **101**, 1836 (1997).
20. M. J. S. Dewar, E. G. Zoebisch, E. F. Healy, and J. J. P. Stewart, *J. Am. Chem. Soc.*, **107**, 3902 (1985).
21. G. Rauhut, A. Alex, J. Chandrasekhar, T. Steinke, W. Sauer, B. Beck, M. Hutter, P. Gedeck, and T. Clark, *VAMP6.1*, Oxford Molecular Ltd., Oxford, 1997.
22. H. Lanig, R. König, and T. Clark, *TRAMP1.1b*, Erlangen, 1995.
23. L. Onsager, *J. Am. Chem. Soc.*, **58**, 1486 (1936).
24. C. J. F. Böttcher, *Theory of Electric Polarisation, Vol. I.*, Elsevier, Amsterdam, 1973, p153.
25. D. Majumdar, R. Sen, K. Bhattacharyya, and S. P. Bhattacharyya, *J. Phys. Chem.*, **95**, 4324 (1991).
26. G. Rauhut, T. Clark, and T. Steinke, *J. Am. Chem. Soc.*, **115**, 9174 (1993).
27. T. Clark, In *Recent Experimental and Computational Advances in Molecular Spectroscopy*, R. Fausto, Ed., Kluwer, Dordrecht, 1992, p. 369.
28. K. Rechthaler, personal communication.
29. D. Piorun, A. B. J. Parusel, K. Rechthaler, K. Rotkiewicz, and G. Köhler, *Chem. Phys. Lett.* (in press).